ICAST2011 #083

# Hybrid Shape Memory Alloy Composites for Extreme Environments

Brian T. Lester[1], Yves Chemisky[1], Andrew B. Geltmacker[2], Siddiq M. Qidwai[2], Richard K. Everett[2], and Dimitris C. Lagoudas[1*]

[1]Department of Aerospace Engineering, Texas A&M University, College Station, TX 77843 USA
[2]Material Science and Technology Division, Code 6300, Naval Research Laboratory, Washington, DC 20375-5343 USA

**Abstract**

The capability of Shape Memory Alloys (SMAs) to generate a residual stress state in a new hybrid SMA-ceramic composite for extreme environments is explored here. By generating a compressive residual stress on the ceramic phase, the beneficial material response observed under compression may be utilized. Specifically a SMA-MAX phase composite with a heterogeneous, irregular microstructure is considered. To incorporate the effects of the microstructure, a numerical model of a realistic microstructure is generated through the results of x-ray tomography and converted into a Finite Element (FE) mesh. A recent phenomenological model for the constitutive behavior of SMAs is then used to describe the response of that phase while an elastic-plastic approximation is used for the MAX phase behavior. The composite is subjected to an actuation (isobaric) loading path. It is shown that through such a loading path, martensitic transformation generates irrecoverable strains in the ceramic phase which results in compressive residual stress state upon unloading. By comparing with the results of a purely thermal or mechanical loading path, the necessity of using SMA transformation through a thermomechanical loading path is demonstrated.

Keywords: Shape Memory Alloys, Composites, Virtual Processing, Martensitic Transformation, Image Based Modeling.

## 1. INTRODUCTION

Shape Memory Alloys (SMAs), which exhibit large strains (~5%) due to a reversible and diffusion-less solid-to-solid phase transformation, have been finding increased implementation in the past 20 years in various industries (Lagoudas (2)). The widest usage to date has been in the biomedical field where the biocompatibility of NiTi SMAs allows for implementation as coronary stents (Migliavacca et. al. (2)). Designers are increasingly, however, taking advantage of the shape memory effect to develop SMA actuators, which have the advantage of being a single piece component (versus multi-piece hydraulic actuators) and can thus be located in environments not previously accessible. SMA actuators can also be found in the aerospace (Hartl and Lagoudas (3)) and petroleum (Anderson et. al. (4)) industries. An

* Address all correspondence to this author: lagoudas@aero.tamu.edu

# Report Documentation Page

*Form Approved*
*OMB No. 0704-0188*



| 1. REPORT DATE | 2. REPORT TYPE | 3. DATES COVERED |
|---|---|---|
| **OCT 2011** | **N/A** | **-** |

4. TITLE AND SUBTITLE
**Hybrid Shape Memory Alloy Composites for Extreme Environments**

5a. CONTRACT NUMBER
5b. GRANT NUMBER
5c. PROGRAM ELEMENT NUMBER

6. AUTHOR(S)

5d. PROJECT NUMBER
5e. TASK NUMBER
5f. WORK UNIT NUMBER

7. PERFORMING ORGANIZATION NAME(S) AND ADDRESS(ES)
**Department of Aerospace Engineering, Texas A&M University, College Station, TX 77843 USA**

8. PERFORMING ORGANIZATION REPORT NUMBER

9. SPONSORING/MONITORING AGENCY NAME(S) AND ADDRESS(ES)

10. SPONSOR/MONITOR'S ACRONYM(S)
11. SPONSOR/MONITOR'S REPORT NUMBER(S)

12. DISTRIBUTION/AVAILABILITY STATEMENT
**Approved for public release, distribution unlimited**

13. SUPPLEMENTARY NOTES
**See also ADA569115. EOARD CSP-11-5077. International Conference on Adaptive Structures and Technologies (22nd) (ICAST2011) Held in Corfu, Greece on October 10-12, 2011. U.S. Government or Federal Purpose Rights License., The original document contains color images.**

14. ABSTRACT
**ThThe capability of Shape Memory Alloys (SMAs) to generate a residual stress state in a new hybrid SMAceramic composite for extreme environments is explored here. By generating a compressive residual stress on the ceramic phase, the beneficial material response observed under compression may be utilized. Specifically a SMA-MAX phase composite with a heterogeneous, irregular microstructure is considered. To incorporate the effects of the microstructure, a numerical model of a realistic microstructure is generated through the results of x-ray tomography and converted into a Finite Element (FE) mesh. A recent phenomenological model for the constitutive behavior of SMAs is then used to describe the response of that phase while an elastic-plastic approximation is used for the MAX phase behavior. The composite is subjected to an actuation (isobaric) loading path. It is shown that through such a loading path, martensitic transformation generates irrecoverable strains in the ceramic phase which results in compressive residual stress state upon unloading. By comparing with the results of a purely thermal or mechanical loading path, the necessity of using SMA transformation through a thermomechanical loading path is demonstrated.**

15. SUBJECT TERMS

| 16. SECURITY CLASSIFICATION OF: | | | 17. LIMITATION OF ABSTRACT | 18. NUMBER OF PAGES | 19a. NAME OF RESPONSIBLE PERSON |
|---|---|---|---|---|---|
| a. REPORT | b. ABSTRACT | c. THIS PAGE | | | |
| **unclassified** | **unclassified** | **unclassified** | **SAR** | **10** | |

example is the Variable Geometry Chevron (VGC) where chevrons with SMA actuators are used for noise suppression of the engine exhaust (Hartl et. al. (5); Hartl et. al. (6)).

As the understanding of SMA actuators continues to expand, they are being proposed to solve increasingly complex engineering problems. One such possibility is the usage of SMAs in high-temperature applications found in the petroleum and aerospace industries. In the case of the petroleum industry, High Temperature Shape Memory Alloys (HTSMAs) (Kumar et. al. (7); Kumar and Lagoudas (8); Lagoudas et. al. (9)) have been investigated for use as down-hole actuators and couplers. Some aerospace applications, however, can require that the SMA component not only actuate but also serve as a thermal insulation layer. Such instances include the leading edge of the aircraft, which during high-speed or altitude flight conditions may experience high temperature conditions, or in the aircraft engine. Consequently, to address such areas, a new functionally graded hybrid SMA-ceramic composite is being investigated. The ability to produce this new composite is a result of the development of new manufacturing techniques for hybrid composites. For example, new techniques have been used to develop TiC-NiTi (SHS and quasi-isostatic pressing) (Strutt et. al. (10)), InSn-CuAlNi (powder-metallurgy) (Barrado et. al. (11)), Al-NiTi (Porter et. al. (12)}, and Mg-NiTi (pressureless infiltration) (Li et. al. (13)) composites. Generally, these composites have an irregular, heterogeneous microstructure for which the effect on the composite transformation characteristics has not been determined. Such effects can be pronounced as a recent micromechanical investigation of ellipsoidal SMA inhomogeneities in stiff matrices has shown that SMA transformation leads to a stress redistribution between the phases creating a reduction in the effective transformation strain and development of anisotropic yield surfaces (Lester et. al. (14)).

Another possible benefit of incorporating SMAs in a hybrid composite is to use martensitic transformation to develop a residual stress state in the composite that puts the ceramic phase under a compressive loading. In generating such a stress state, the superior mechanical properties of the ceramic phase will be utilized. Past numerical investigations on SMA fibers in an elasto-plastic aluminum matrix have shown that a residual stress state is developed due to yielding of the matrix phase (Auricchio and Petrini (15); Freed and Aboudi (16)). To investigate similar effects in the proposed composite, a unique group of ceramics - MAX phases (Barsoum (17); Barsoum and El-Raghy (18)) - are utilized. Such ceramics exhibit a repeatable, non-linear and hysteretic response under mechanical loading due to the formation of incipient kink bands (Barsoum et. al. (19)). Interestingly, however, such MAX phases also exhibit the capability to produce irrecoverable strains due to the kink band propagation and have even been observed to have ductile-like behavior at room temperature under compression (Barsoum and El-Raghy (20)).

In the current work, the capability of the proposed SMA-MAX phase composite to develop a compressive residual stress state on the ceramic phase is investigated. To consider the effects of the heterogeneous, irregular microstructure (which have not been previously considered), a numerical model of a *realistic* microstructure is generated from x-ray tomography. By then using a recent 3D phenomenological SMA model and a simplified representation of the MAX phase response, the composite is virtually processed through an actuation loading path. The response of the composite through such loadings is explored to determine if the desired residual stress state is generated and how the interactions between the two phases interact.

## 2. NUMERICAL MICROSTRUCTURE GENERATION AND MODELING APPROACH

To account for the influences of an irregular microstructure, a numerical model based on actual microstructures is necessary. To this end, an image-based technique which develops numerical microstructures from x-ray tomography results is utilized. These techniques have been used to analyze of a wide variety of material responses (e.g., yield in polycrystalline β-Ti (Qidwai et. al. (21))) incorporating

the 3D effects of the microstructure. The basis of this technique is first identifying and characterizing an appropriate microstructure. To identify such a microstructure, it is noted that one of the most promising manufacturing techniques for such hybrid composites is the infiltration technique used by Li et. al. to make a Mg-NiTi composite (Li et. al. (13)). This technique first manufactures a base specimen with sufficiently high open porosity and then infiltrates the second phase into the porosity. Therefore, a porous NiTi specimen was selected for use as the base microstructure as a SMA-MAX phase composite was not available. A SkyScan 1172 x-ray tomograph was used to characterize the microstructure of the selected specimen. The porosity was then treated as the MAX phase to simulate complete infiltration of the base specimen. A 2D tomography and reconstructed 3D numerical microstructure are shown in Figs. 1a and b, respectively. The numerical microstructure was then turned into a Finite Element (FE) mesh by treating each volume pixel (voxel) of the numerical microstructure as a 3D linear element. A voxel sampling was used to create a FE mesh that had a reasonable computational cost while maintaining geometric fidelity. The FE mesh used in this study is then presented in Fig. 1c. The resultant mesh is comprised of 48% MAX phase.

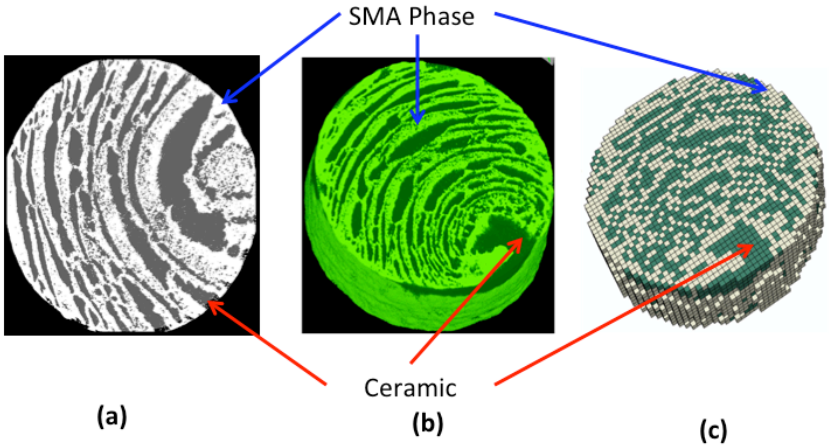


**Figure 1.** Numerical Microstructure and mesh generation of a NiTi-MAX phase composite: (a) segmented 2D x-ray tomograpy of the characterized porous NiTi cross-section (b) reconstructed 3D microstructure of the considered composite and (c) the finite element mesh of the composite

The considered composite is virtually processed through a actuation (isobaric) loading path. First, a mechanical load of 200 MPa is applied to the cylindrical specimen in the axial ("3") direction at 500°C. This start temperature is utilized as it is a common annealing temperature for SMAs and thus cooling the composite incorporates the effects of thermal expansion mismatch. The composite is then cooled, holding the applied load constant, below the martensitic finish ($M_f$) temperature to undergo complete forward (austenite to martensite) transformation and then heated back to 500°C ensuring that the SMA completes reverse transformation and returns to the original temperature. The composite is then unloaded. Such an actuation loading path is shown schematically in the stress-temperature space in Fig. 2 with a representative bulk SMA phase diagram superimposed for comparison purposes.

To describe the constitutive response of the SMA phase, a recent 3D phenomenological model derived from continuum thermodynamics developed by Lagoudas et. al. (Lagoudas et. al. (22)) is utilized which is an extension of the Unified Model previously discussed by Lagoudas and collaborators (Lagoudas et. al.(23)). The SMA considered is a Ni-rich (60 wt %) NiTi whose relevant modeling parameters were determined by Hartl et. al. (Hartl et. al. (5);Hartl et. al. (6)). The MAX phase is taken to be $Ti_2AlC$ and the relevant thermoelastic and transformation characteristics of the two phases are given in Appendix A. MAX phases have been referred to as kinking non-linear elastic solids (Barsoum and Basu (24)) due to their repeatable, non-linear and hysteretic response (Barsoum et. al. (19)). Although a microscale model has been proposed to describe the behavior of these materials (Barsoum et. al. (25)), there is currently a lack of 3D macroscale models which are implementable in a FE framework. Instead, the macroscale models currently found in the literature are 1D with complicated methods of incorporating the material history dependence (Zh

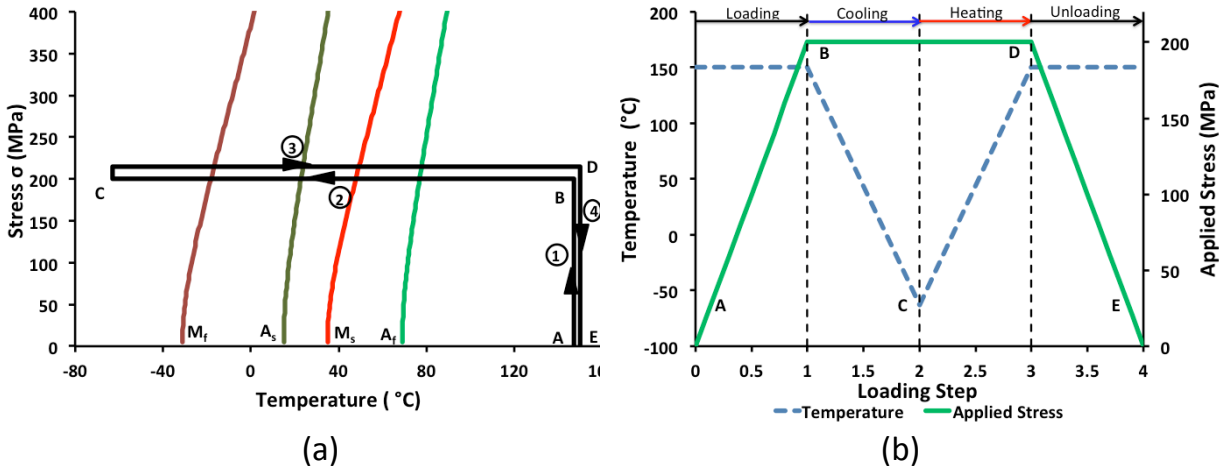


**Figure 2.** Considered isobaric (actuation) loading path (a) in the stress-temperature space overlayed on the bulk SMA phase diagram and (b) the applied stress and temperature through loading

ou et. al. (26); Kalidindi et. al. (27)). As the 3D behavior is of interest in this study and a macroscale model is still in development, a simplification of the MAX phase behavior is necessary. Specifically, to investigate whether a compressive residual stress state can be developed through the development of irrecoverable strains, an elasto-plastic approximation to the MAX phase response is utilized. To this end, it is noted that open hysteresis loops have been observed under tensile loading at room temperature by Radovic et. al. (Radovic et. al. (28)) when the MAX phase is loaded above 200 MPa indicating a plastic response. Thus, for this study, the isotropic plasticity model of ABAQUS is used assuming a yield stress of 200 MPa and incorporating a high plastic-hardening to represent the open-hysteresis plasticity. The 1D elasto-plastic curve used for ABAQUS input is presented in Appendix A Fig. 7.

## 3. RESULTS AND DISCUSSION

The ability of an SMA to generate a compressive residual stress state in an SMA-MAX phase composite through martensitic transformation is explored here. The stress states of the $Ti_2AlC$ phase in the direction of applied (axial) loading, $\sigma_{33}$, at the points labeled A-E in Fig. 2 are shown in Fig. 3. For clarity, the SMA phase has been removed. Initially, at point A in Fig. 2, the composite is unloaded and the MAX phase is stress free (Fig. 3a). After mechanical loading at 500°C, point B in Fig. 2, the ceramic phase has a tensile stress state in the direction of applied loading with areas of high local ceramic content having lower stresses than areas of higher SMA content as observed in Fig. 3b. After the composite is cooled (Fig. 2 point C), the MAX phase, as shown in Fig. 3c, has an increased stress in the direction of applied loading. After the composite is subsequently heated back to 500°C (point D), a large reduction in the $Ti_2AlC$ stress is noted in Fig. 3d. Finally, after mechanically unloading (point E), the composite returns to its initial external loading state although the ceramic phase has a residual stress state which is mostly compressive as shown in Fig. 3e. Importantly, by comparing points with the same external loading conditions (points A and E and points B and D) different ceramic stress states are observed in the corresponding figures in Fig. 3. In both cases, the difference between the two points is the effect of the thermal cycle through forward and reverse transformation.

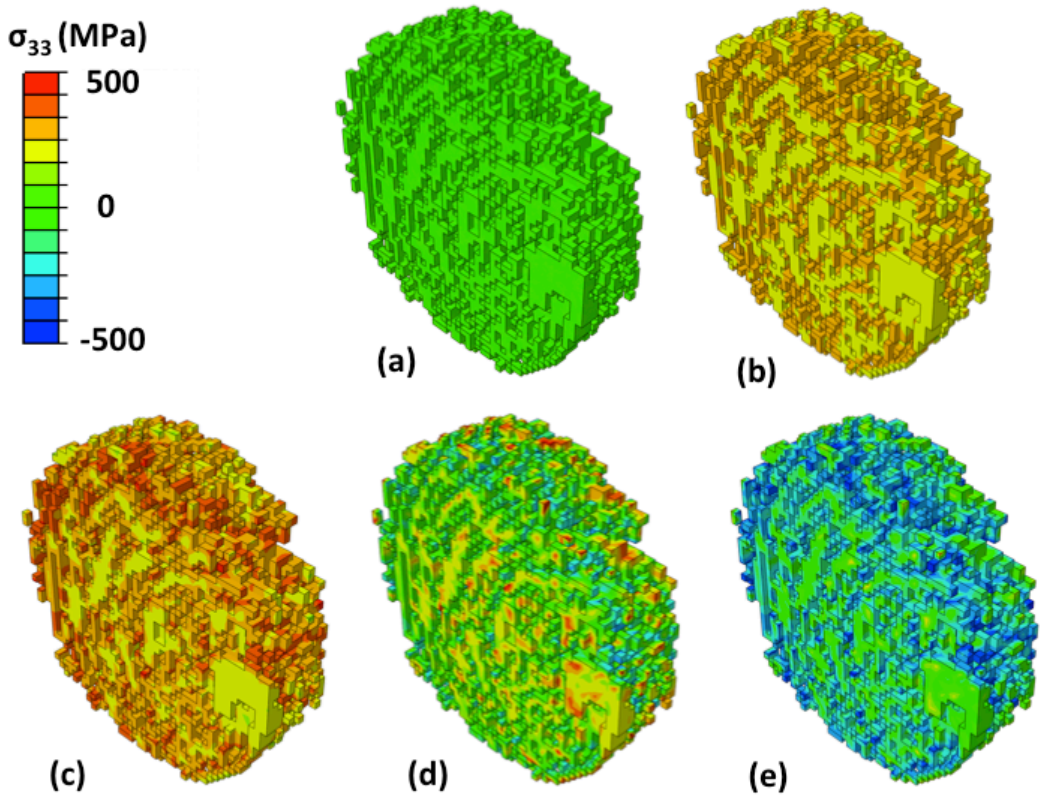


**Figure 3.** Stress state in the Ti2AlC phase in the direction of applied loading ("3") through an actuation loading path under 200 MPa applied load (SMA phase has been removed for clarity): (a) at the beginning of the loading cycle (b) after mechanical loading (c) after cooling through forward transformation (d) following heating through reverse transformation and (e) subsequent to mechanical unloading

From the results of Fig. 3, it is demonstrated that a residual stress state does develop in the composite through a thermomechanical loading cycle incorporating complete transformation. Processing through such a cycle, however, does not prove that such a loading path is necessary to yield the desired results. If a simpler loading path, e.g. purely mechanical or purely thermal, can produce a similar residual stress state operational conditions may continually produce damage leading to failure. Furthermore, if a simpler loading path may be utilized, an SMA metal phase may be unnecessary. To consider this issue, the final stress states in the direction of applied loading are presented below in Fig. 4 for the previous thermomechanical and pure mechanical and thermal loading paths. For the cases of the pure thermal or mechanical loading, it is observed in Figs. 4a and c that neither loading path produces a negligible residual stress state. Thus, to produce a residual stress state a coupled thermomechanical loading path is necessary. As such, by careful consideration of the desired operational conditions of the material, a thermomechanical loading path may be designed resulting in a compressive residual stress state.

Although the ability to generate a residual stress state, which qualitatively appears compressive, through an actuation cycle has been demonstrated, it has not been quantitatively considered. To this end, Fig. 5 presents the $Ti_2AlC$ phase average stress in the direction of applied loading, $\bar{\sigma}_{33}$, along with the average SMA martensitic volume fraction (MVF), $\xi$. It is observed in Fig. 5 that during step 1, the mechanical loading corresponding to A➔B in Fig. 2, the response is initially elastic although at higher stresses there is a small change in slope indicating the beginning of irrecoverable strain generation. During the initial cooling of step 2 (B➔C of Fig. 2), prior to the initiation of forward transformation, the average stress in the direction of loading decreases due to thermal expansion mismatch of the two constituent phases. During forward transformation, as indicated by the increase in SMA phase average Martensitic Volume Fraction (MVF), $\xi$, a sharp rise of nearly 100 MPa is noted in the $Ti_2AlC$ phase. Upon the completion of transformation, a further reduction in the phase average stress in the direction of applied loading is observed as the composite is further cooled. During the heating stage, step 3 in Fig. 5 corresponding to C➔D in Fig. 2, the thermal expansion mismatch yields higher MAX phase average stress in the direction of applied loading. When the SMA phase undergoes reverse transformation, indicated by the SMA phase average MVF going to 0, a large drop of over 200 MPa is noted in the ceramic phase as the SMA contracts allowing for a stress relaxation in the MAX phase. As the composite is heated back to the original temperature, the phase average ceramic stress in the direction of applied loading continues to increase. At the end of the heating step, point D in Fig. 2, the ceramic has a lower phase average stress that at the same point (B) prior to transformation. Thus, when the composite is unloaded during Step 4

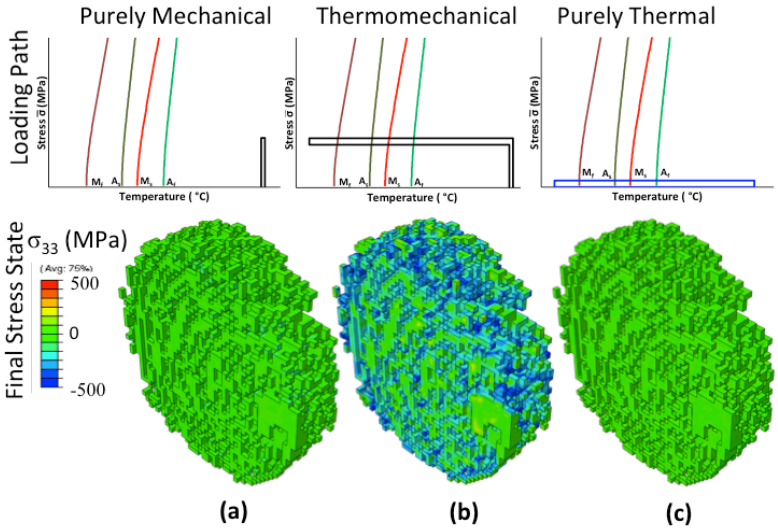


**Figure 4.** Effect of load path on the final residual stress state of the considered SMA-MAX phase composite. The top row shows the different considered loading paths while the bottom row shows the final stress in the direction of applied loading of the MAX phase following the completion of the (a) purely mechanical (b) thermomechanical and (c) purely thermal loading paths

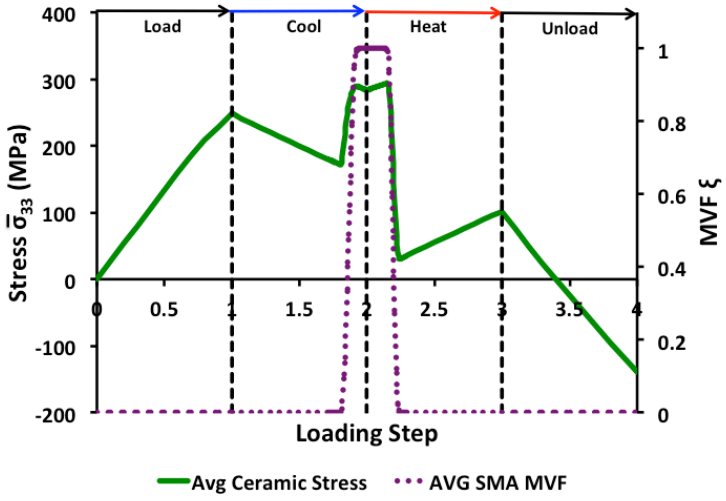


**Figure 5.** Phase average stress of the MAX phase in the direction of applied loading over the course of the loading cycle

(D➔E) the MAX phase average stress in the direction of applied loading decreases past zero and achieves a final average stress of -140 MPa.

As the previously discussion has indicated, the composite residual stress state in the composite develops from the generation of irrecoverable strains in the MAX phase. To consider the evolution of such strains over the course of the loading cycle, the ceramic phase average irrecoverable strain in the direction of applied loading, $\bar{\varepsilon}^{p}_{33}$, is presented in Fig. 6 along with the SMA phase average MVF. During the mechanical loading of step 1 in Fig. 6, it is noted that the response is initially elastic although towards the end of the loading step some irrecoverable strains are generated. During cooling, step 2, prior to forward transformation a small increase in the average irrecoverable strain in the direction of applied loading is observed. When forward transformation occurs, a much larger quantity of irrecoverable strains are generated in the direction of applied loading. Small amounts of irrecoverable strain are generated during further cooling of step 2 and the initial heating of step 3 prior to reverse transformation as observed in Fig. 6. Through reverse transformation, a small amount of irrecoverable strains in the direction opposite of loading are generating leading to a decrease in the magnitude of irrecoverable strain in the direction of loading as noted in Fig. 6. These strains are the result of local effects and highlight the importance of microstructure in such composites as incorporation of specific features through microstructure design could be used to increase or decrease such effects. Over the course of further cooling, minor decreases in the magnitude of irrecoverable strain in the direction of loading are observed in Fig. 6. By mechanically unloading the composite, step 4 in Fig. 6, a more substantial decrease in the magnitude of the plastic strains in the direction of applied loading is noted although such reductions are much smaller than the amount of strain generated during forward transformation. The final irrecoverable strain magnitude in the direction of applied loading of ≈0.3%.

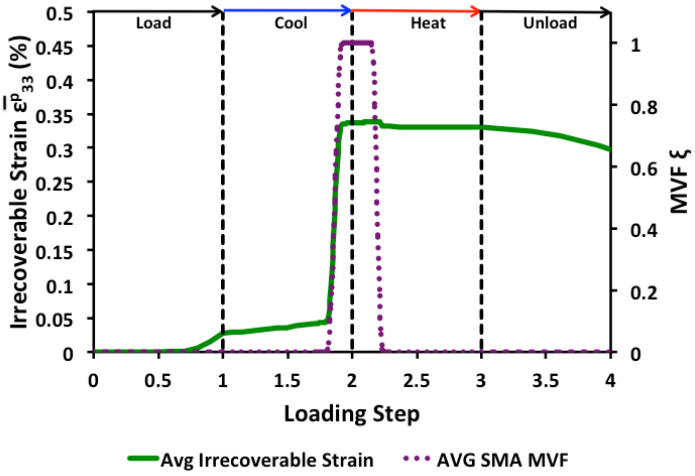


**Figure 6.** Phase average irrecoverable strain of the MAX phase in the direction of applied loading over the course of the loading cycle

## 4. CONCLUSION

A new hybrid SMA-MAX phase composite under development for use in extreme environment applications was investigated. Specifically, a numerical model was developed incorporating the effects of a realistic microstructure by using x-ray tomography and other image-based modeling techniques. By then making simplifying assumptions in regards to the MAX-phase behavior, an elasto-plastic response was used to approximate the MAX phase behavior. Through an actuation loading path, it was demonstrated that transformation may be used to develop a residual stress state in the composite. Specifically, a compressive residual load was placed on the MAX phase to take advantage of it beneficial mechanical properties. Through such a thermomechanical cycle, it was shown that the cause of such a residual stress state is the generation of irrecoverable strains in the MAX phase due to increased stresses from SMA martensitic transformation. Such a residual stress state could not be developed through a

purely thermal or mechanical loading path demonstrating the capability of SMAs to be used to tailor residual stress states of composites.

## Acknowledgements

This work was supported by AFOSR under MURI contract C09-00931 and the authors would like to thank the program manager Dr. David Stargel. Also, the support of the NSF International Institute of Materials for Energy Conversion (IIMEC), award #0844082, the basic research program of the Naval Research Laboratory, and the DoD High Performance Computing network is acknowledged.

## References

1. Lagoudas, D., ed., *Shape Memory Alloys: Modeling and Engineering Analysis*, Springer-Verlag, New York.
2. Migliavacca, F., Petrini, L., Colombo, M., Auricchio, F., and Pietrabissa, R., "Mechanical Behavior of Coronary Stents Investigated through the Finite Element Method," *Journal of Biomechanics*, Vol. 35, 2002, pp. 803-811.
3. Hartl, D. J., and Lagoudas, D., "Aerospace Applications of Shape Memory Alloys," *Proceedings of the Institution of Mechanical Engineers, Part G: Journal of Aerospace Engineering*, Vol. 221 (Special Issue), 2007, pp. 535-552.
4. Anderson, A., Pedersen, D., Sivertsen, A., and Sangesland, S., "Detailed Study of Shape Memory Alloys in Oil Well Applications," Sintef Petroleum Research, 1999, Trondheim, Norway.
5. Hartl, D. J., Lagoudas, D., Mabe, J., Calkins, F., and Mooney, J., "Use of Ni60Ti Shape Memory Alloy for Active Jet Engine Chevron Applications, Part I: Thermomechanical Characterization," *Smart Materials and Structures*, Vol. 19, No. 1., 2009.
6. Hartl, D. J., Lagoudas, D., Mabe, J., Calkins, F., and Mooney, J., "Use of Ni60Ti Shape Memory Alloy for Active Jet Engine Chevron Applications, Part II: Experimentally Validated Numerical Analysis," *Smart Materials and Structures*, Vol. 19, No. 1., 2009.
7. Kumar, P. K., Lagoudas, D. C., Zanca, K. J., and Lagoudas, M. Z., "Thermomechanical Characterization of High Temperature SMA Actuators," *Proceedings of SPIE*, Vol. 6170, 2006, pp. 306-312.
8. Kumar, P. K., and Lagoudas, D. C., "Experimental and Microstructural Characterization of Simultaneous Creep, Plasticity and Phase Transformation in $Ti_{50}Pd_{40}Ni_{10}$ High-Temperature Shape Memory Alloy," *Acta Materialia*, Vol. 58, 2010, pp, 1618-1628.
9. Lagoudas, D. C., Chatzigeorgiou, G., and Kumar, P. K., "Modeling and Experimental Study of Simultaneous Creep and Transformation in Polycrystalline High-Temperature Shape Memory Alloys," *Journal of Intelligent Material Systems and Structures*, Vol. 20, 2009, pp. 2257-2267.
10. Strutt, E. R., Olevsky, E. A., and Meyers, M. A., "Combustion Synthesis/Quasi-Isostatic Pressing of TiC-NiTi Cermets: Processing and Mechanical Response", *Journal of Materials Science*, Vol. 43, 2008, pp. 6513-6526.
11. Barrado, M., Lopez, G. A., No, M. L., and San Juan, J., "Composites with Ultra High Damping Capacity Based on Powder Metallurgy Shape Memory Alloys," *Material Science & Engineering A*, Vol. 521-522, 2009, pp. 363-367.

12. Porter, G. A., Liaw, P. K., Tiegs, T. N., and Wu, K. H., "Ni-Ti SMA-Reinforced Al Composites," *Journal of the Minerals, Metals, and Materials Society,* Vol. 52, No. 10, 2000, pp. 52-56.
13. Li., D. S., Zhang, X. P., and Mai, Y. W., "Lightweight NiTi Shape Memory Alloy Based Composites with High Damping Capacity and High Strength," *Journal of Alloys and Compounds*, Vol. 490, pp. L15-L19.
14. Lester, B. T., Chemisky, Y., and Lagoudas, D. C., "Transformation Characteristics of SMA Composites", *Smart Materials and Structures*, Vol. 20, 2011, 094002.
15. Auricchio, F., and Petrini, L., "A Three-Dimensional Model Describing Stress-Temperature Induced Solid Phase Transformations: Thermomechanical Coupling and Hybrid Composite Applications," *International Journal for Numerical Methods in Engineering,* Vol. 61, 2004, pp. 716-737.
16. Freed, Y., and Aboudi, J., "Thermomechanically Coupled Micromechanical Analysis of Shape Memory Alloy Composites undergoing Transformation Induced Plasticity," *Journal of Intelligent Material Systems and Structures*, Vol. 20, 2009, pp. 716-737.
17. Barsoum, M. W., "The $M_{N+1}AX_N$ Phases: A New Class of Solids; Thermodynamically Stable Nanolaminates," *Progress in Solid State Chemistry*, Vol. 28, 2000, pp. 201-281.
18. Barsoum, M. W., and El-Raghy, T., "The MAX Phases: Unique Carbide and Nitride Materials: Tertiary Ceramics are Soft and Machinable, yet Heat-Tolerant, Strong and Lightweight," *American Scientist*, Vol. 89, 2001, pp. 334-343.
19. Barsoum, M. W., Zhen, T., Kalidindi, S. R., Radovic, M., and Murugaiah, A., "Fully Reversible, Dislocation-Based Compressive Deformation of $Ti_3SiC_2$ to 1 GPa," *Nature Materials*, Vol. 2, 2003, pp. 107-111.
20. Barsoum, M. W., and El-Raghy, T., "Room-Temperature Ductile Carbides," *Metallurgical and Material Transactions A*, Vol. 30A, 1999, pp. 363-369.
21. Qidwai, M. A. S., Lewis, A. C., and Geltmacher, A. B., "Using Image-Based Computational Modeling to Study Microstructure-Yield Correlations in Metals," *Acta Materialia*, Vol. 57, 2009, pp. 4233-4247.
22. Lagoudas, D., Hartl, D., Chemisky, Y., Machado, L., and Popov, P., "Constitutive Model for the Numerical Analysis of Phase Transformation in Polycrystalline Shape Memory Alloys," *International Journal of Plasticity*, 2011, Submitted.
23. Lagoudas, D. C., Bo, Z., and Qidwai, M. A., "A Unified Thermodynamic Constitutive Model for SMA and Finite Element Analysis of Active Metal Matrix Composites," *Mechanics of Composite Materials and Structures*, Vol. 3, 1996, pp. 153-179.
24. Barsoum, M. W., and Basu, S., "Kinking Nonlinear Elastic Solids," *Encyclopedia of Materials: Science and Technology*, 2010, pp. 1-23.
25. Barsoum, M. W., Zhen, T., Zhou, A., Basu, S., and Kalidindi, S. R., "Microscale Modeling of Kinking Nonlinear Elastic Solids," *Physical Review B*, Vol. 71, 2005, 134101.
26. Zhou, A. G., Basu, S., Friedman, G., Finkel, P., Yeheskel, O., and Barsoum, M. W., "Hysteresis in Kinking Non-linear Elastic Solids and the Preisarch-Mayergoyz Model," *Physical Review B*, Vol. 82, 2010, 094105.
27. Kalidindi, S. R., Zhen, T., and Barsoum, M. W., "Macroscale Constitutive Modeling of Kinking Nonlinear Elastic Solids," *Material Science & Engineering A*, Vol. 418, 2006, pp. 95-98.
28. Radovic, M., Barsoum, M. W., El-Raghy, T., Weiderhorn, S. M., and Luecke, W. E., "Effect of Temperature, Strain Rate and Grain Size on the Mechanical Response of $Ti_3SiC_2$ in Tension," *Acta Materialia*, Vol. 50, 2002, pp. 453-459.
29. Radovic, M., Barsoum, M. W., Ganguly, A., Zhen, T., Finkel, P., Kalidindi, S. R., and Lara-Curzio, E., "On the Elastic and Mechanical Damping of $Ti_3SiC_2$, $Ti_3GeC_2$, $Ti_3Si_{0.5}Al_{0.5}C_2$, and $Ti_2AlC$ in the 300-1573 K Temperature Range," *Acta Materialia*, Vol. 54, 2006, pp. 2757-2767.
30. Barsoum, M. W., Ali, M., and El-Raghy, T., "Processing and Characterization of $Ti_2AlC$, $Ti_2AlN$, and $Ti_2AlC_{0.5}N_{0.5}$," *Metallurgical and Material Transactions A*, Vol. 31A, 2000, pp.1857-1865.

## Appendix A

**Table 1.** Model Parameters for Ni60Ti40 (wt%) (Hartl et. al. (6))

| $E_A$ | $E_M$ | $\nu^M = \nu^A$ | $\alpha^M = \alpha^A$ | $M_s$ | $M_f$ | $A_s$ | $A_f$ | $H_{MAX}$ |
|---|---|---|---|---|---|---|---|---|
| 90 GPa | 63 GPa | 0.33 | $10x10^{-6}°C^{-1}$ | 35°C | -31°C | 15°C | 69°C | 0.0158 |

**Table 2.** Material Properties for the ceramic matrix – $Ti_2AlC$ (Radovic et. al. (29))

| E | ν | α† |
|---|---|---|
| 278 GPa | 0.17 | $8.20x10^{-6}°C^{-1}$ |

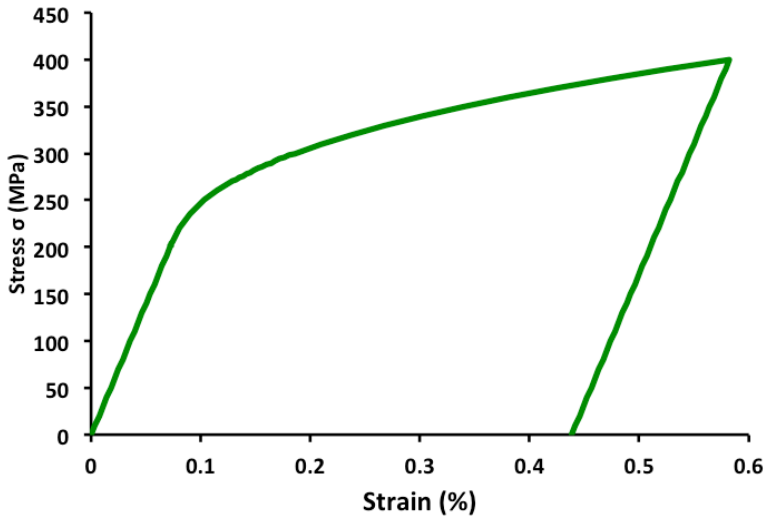


**Figure 7.** Elastic-Plastic response assumed for the MAX phase behavior

† Value taken from Barsoum et. al. (30)